sciendo

Acta Pharm. **74** (2024) 61–79
https://doi.org/10.2478/acph-2024-0004

Original research paper

Furanocoumarin compounds isolated from *Dorstenia foetida* potentiate irinotecan anticancer activity against colorectal cancer cells

SUPUSSON PENGNAM[1]
WATCHARAPA JITKAROON[2]
ROONGTIWA SRISUPHAN[3]
PAWARIS WONGPRAYOON[4]
KANOK-ON RAYANIL[2]
PURIN CHAROENSUKSAI[4,*]

[1] *Department of Biomedicine and Health Informatics, Green Innovations Group (PDGIG), Faculty of Pharmacy Silpakorn University, Nakhon Pathom 73000, Thailand*

[2] *Department of Chemistry, Faculty of Science, Silpakorn University, Nakhon Pathom, 73000, Thailand*

[3] *Bioactives from Natural Resources Research Collaboration for Excellence in Pharmaceutical Sciences (BNEP) Faculty of Pharmacy, Silpakorn University, Nakhon Pathom 73000 Thailand*

[4] *Department of Biomedicine and Health Informatics and Bioactives from Natural Resources Research Collaboration for Excellence in Pharmaceutical Sciences (BNEP), Faculty of Pharmacy, Silpakorn University, Nakhon Pathom 73000 Thailand*

Accepted October 3, 2023
Published online October 5, 2023

ABSTRACT

Although the anticancer activity of *Dorstenia foetida* was already observed, the chemical entity responsible for this activity remained unidentified. In this study, the cytotoxic activity of two furanocoumarin compounds, *i.e.*, 5-methoxy-3-(3-methyl-2,3-dihydroxybutyl)-psoralen (**1**) and 5-methoxy-3-(3-methyl-2,3-dihydroxybutyl)-psoralen diacetate (**2**) isolated from ethyl acetate fraction of *D. foetida* (whole plant) was investigated in several cancer cell lines including HN22, MDA-MB-231, HCT116, and HT29. The results revealed that compound **2** exhibited cytotoxic activity, particularly against colorectal cancer cell lines HCT116 and HT29. The interplay between compound **2** and irinotecan (Iri) showed synergism against HCT116, which was analyzed by CompuSyn software. The simulation revealed that, at the molar ratio of Iri:**2** of 1:40, the concentration predicted to achieve a 90 % inhibitory effect when used in the combination would be ~28- and ~4-fold lower than the concentration of compound **2** and Iri, resp., when used individually. Finally, the percentage of apoptotic cells in the HCT116 line treated with the combination was markedly higher than in the cells treated with the individual agent (60 % apoptotic cells for the combination compared to 17 and 45 % for Iri and compound **2** monotherapy, resp). In conclusion, our results identified compound **2** as a plant-derived compound exhibiting anticancer properties that can act synergistically with Iri and warranted further research to assess the potential of this synergism for colorectal cancer treatment.

Keywords: 5-methoxy-3-(3-methyl-2,3-dihydroxybutyl)-psoralen diacetate, furanocoumarins, anticancer activity, irinotecan, synergism

INTRODUCTION

Cancer is a disease resulting from genetic abnormalities which culminate in the dysregulation of cell functions. Cancerous cells exhibit key altered characteristics compared

*Correspondence; e-mail: charoensuksai_p@su.ac.th

to normal cells, *i.e.*, uncontrolled cell division, avoidance of cell death, invasion of neighboring tissues, and spread to distant organs by metastasis (1). Given the time-consuming nature of the accumulation of genetic defects that drive carcinogenesis, it is not surprising that the rate of cancer occurrence increases with age (2). Therefore, the burden of cancer disease can be expected to escalate in many countries facing, or transitioning into, an aging society with a high proportion of elderly citizens.

Pharmacological management of cancers using a monotherapy strategy is generally associated with two major limitations. Firstly, cancer cells often harbor abnormalities in multiple molecular pathways. Inhibiting one pathway with an anticancer agent often results in a limited response. Secondly, to achieve a sufficient inhibitory effect, a high dose is often required which can lead to a higher rate of adverse events (3, 4). At present, pharmacological management of cancers often employs multiple drugs in combination therapy. This strategy benefits from the synergy of the anticancer agents which generally leads to a higher probability of achieving a favorable response, lessening concentration-dependent adverse events, as well as minimizing drug resistance (5).

Currently, clinically approved anticancer agents of plant origin include taxol from *Taxus brevifolia*, vinblastine and vincristine from *Catharanthus roseus*, podophyllotoxins – the natural precursor of etoposide – from the wild mandrake *Podophyllum peltatum* and irinotecan (Iri) – the derivative of the alkaloid camptothecin – from *Camptotheca acuminata* (6, 7). Iri, which exerts its anticancer activity through inhibition of topoisomerase I, has been widely used to treat many solid tumors including lung, pancreatic and colorectal cancer (8). For colorectal cancer, Iri is usually used in combination with other drugs such as folinic acid and 5-fluorouracil in the FOLFIRI regimen, or in combination with monoclonal antibodies such as bevacizumab or cetuximab based on disease stage and genetic signature (9).

As a part of the botanical family Moraceae, the genus *Dorstenia* encompasses >170 species. The anticancer activity of plants in the genus *Dorstenia* has been recorded both in folklore remedies and modern research. In Mexico, *D. contrajerva* L. has been used as a herbal medicine for gastrointestinal and skin cancer (10). In Ethiopia, the roots of *D. barnimiana* Schweinf. are used for cancer treatment (11–13). In addition to activity in traditional medicinal records, modern research also provides evidence in support of the anticancer properties of *Dorstenia*. Methanolic extract of *D. elliptica* has been shown to inhibit pancreatic cancer cell line MiaPaCa-2 (14). Ethanolic extract of *D. psilirus* has also been shown to inhibit pancreatic cell line MiaPaCa-2 (IC_{50} ~9 μg mL^{-1}), leukemic cell line CCRF-CEM (IC_{50} ~7 μg mL^{-1}) and suppress angiogenesis (14). Several chemical entities with anticancer properties have been isolated from plants in the genus *Dorstenia*, such as *D. kameruniana, D. brasiliensis, D. mannii, D. poinsettifolia,* including benzofuran, chalcone, furanocumarin, terpenoid and flavonoid which inhibit diverse cancer cell lines including CCRF-CEM, L-1210 (leukemic), HL-60 (leukemia), MDA-MB-231 (breast cancer), HCT116 (colorectal cancer), U87MG (glioblastoma), HepG2 (liver cancer) (15–17). Although the anticancer activities of other members of the *Dorstenia* genus are well-documented, such activity remains largely unknown in *D. foetida*. To our knowledge, only one research article describes the inhibitory activity of *D. foetida n*-heptane extract against the colorectal cancer cell line HT29 and prostatic cancer cell line PC3 (18).

EXPERIMENTAL

Chemicals and reagents

Organic solvents used for plant extraction and chromatography including ethanol, methanol, *n*-hexane, ethyl acetate, and *n*-butanol were purchased from Merck (Germany). Deuterated chloroform ($CDCl_3$, 99.98 % D) for nuclear magnetic resonance (NMR) analysis and cerium(IV) sulfate were purchased from Sigma-Aldrich (USA). Silica gel for column chromatography (0.063–0.2 mm or 0.040–0.063 mm) was purchased from Merck. Precoated silica gel 60 F_{254} plates for analytical thin-layer chromatography (TLC) and preparative TLC were purchased from Merck.

3-(4,5-Dimethylthiazol-2-yl)-2,5-diphenyltetrazoliumbromide (MTT), dimethyl sulfoxide (DMSO), human epithelial growth factor (hEGF), insulin, transferrin and HEPES were purchased from Sigma-Aldrich. Cholera toxin was purchased from MedChemExpress (USA). Hydroxypropyl-β-cyclodextrin (Cavasol W7 HP Pharma) was purchased from Wacker Chemie AG (Germany). Irinotecan 20 mg mL^{-1} concentrate for solution for infusion [20 mg mL^{-1} irinotecan HCl trihydrate + excipients: sorbitol, lactic acid, water for injections, and sodium hydroxide (for pH-adjustment)] was purchased from Fresenius Kabi Oncology (UK). Hoechst 33342 trihydrochloride and SYTOX® green were purchased from Invitrogen (USA).

Plant material

All *D. foetida* plant specimen used for the experiment was propagated in our greenhouse in Bangkok, Thailand. The whole plants of *Dorstenia foetida* were harvested in November 2021. A voucher specimen (SUPY.PC2) was deposited at the Herbarium of the Faculty of Pharmacy, Silpakorn University, Thailand.

Extraction and isolation

The sun-dried and powdered whole plants (both aerial parts and roots) of *D. foetida* (254.6 g) were extracted with 95 % ethanol (3.5 L) at room temperature (3 times for 24 h each). Removal of the solvent under reduced pressure at 40 °C provided a greenish-dark crude ethanolic extract (24.7 g, crude). The crude extract was suspended in water (2.5 L) and successively partitioned with hexane (800 mL × 3), ethyl acetate (800 mL × 3), and *n*-butanol (800 mL × 3). The respective solvents were then evaporated to dryness at 40 °C under reduced pressure to give hexane (dark green oil, 6.4 g, Hex), ethyl acetate (dark green semisolid, 4.8 g, EtOAc), *n*-butanol (brown oil, 4.3 g, BuOH) and water (yellow semisolid, 7.2 g, H_2O) fractions. A portion of crude extract and fractions were dissolved in DMSO and used for the screening of anticancer properties. Subsequently, the EtOAc fraction was selected for further separation.

The EtOAc fraction (4.7 g) was subjected to silica gel column chromatography (CC) and eluted with a hexane-EtOAc gradient system (100:0 to 0:100, *V*/*V*) and finally with pure methanol to obtain 10 subfractions (Fr.1-Fr.10), which were combined after TLC monitoring. Subfraction Fr.4 (0.0457 g) was further purified by preparative TLC with 20 % EtOAc in benzene as the mobile phase to obtain compound **2** (14.7 mg). Fr.6 (0.5070 g) was separated

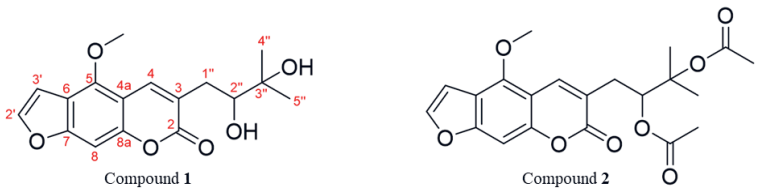


Fig. 1. Chemical structures of compound **1** [5-methoxy-3-(3-methyl-2,3-dihydroxybutyl)-psoralen] and compound **2** [5-methoxy-3-(3-methyl-2,3-dihydroxybutyl)-psoralen diacetate] isolated from EtOAc fraction of *D. foetida* (whole plant) extract.

by silica gel CC and eluted with 20–80 % EtOAc in hexane to afford 6 subfractions (Fr.6.1-Fr.6.6). Subfraction Fr.6.2 (0.1063 mg) was crystallized in EtOH to give compound **1** (19.8 mg). Each portion of compounds **1** and **2** (Fig. 1) was dissolved in a mixture containing DMSO and 30 % (*m*/*V*) hydroxypropyl-β-cyclodextrin (DMSO-HPBCD) and used for the investigation of anticancer properties.

Chemical identification

Ultraviolet (UV) spectra were acquired on a Hewlett Packard 8453 UV-Vis-spectrometer (Agilent Technologies, Germany). ^{1}H and ^{13}C nuclear magnetic resonance (NMR) data were obtained on a Bruker AVANCE 300 MHz spectrometer (Bruker, Switzerland); tetramethylsilane (TMS, Sigma-Aldrich, Germany) was used as an internal standard. High-resolution mass spectra (HRMS) were recorded on a Micro TOF Bruker Daltonic mass spectrometer (Bruker Daltonics, Germany). Identification data are presented in Table I.

Cell cultures

Immortalized human keratinocyte cell line HaCaT was obtained from CLS Cell Lines Service GmbH (Eppelheim, Germany). Colorectal cancer cell lines HCT116 and HT29, breast cancer cell lines MCF7 and MDA-MB-231, hepatocellular carcinoma cell line HepG2 and fetal colonic epithelial cell line FHC were obtained from ATCC (USA). Head-and-neck cancer cell line HN22 was obtained from the Faculty of Dentistry, Naresuan University (Phitsanulok, Thailand). Dulbecco's modified Eagle's medium (DMEM), DMEM/F12, fetal bovine serum (FBS), non-essential amino acids (NEAA), Glutamax, and penicillin/streptomycin (Pen/Strep) solution were purchased from Gibco (USA). Tissue culture plates (96-well and 6-well) were purchased from Corning (USA).

HaCaT, MCF7, and MDA-MB-231 cells were maintained in DMEM supplemented with 10 % FBS and 1 % Pen/Strep. HCT116, HT29, HepG2, and HN22 cells were maintained in DMEM supplemented with 10 % FBS, 1 % NEAA, 1 % Glutamax and 1 % Pen/Strep. FHC cells were maintained in DMEM/F12 supplemented with 10 % FBS, 1 % Pen/Strep, 20 ng mL^{-1} hEGF, 10 ng mL^{-1} cholera toxin, 5 μg mL^{-1} insulin, 5 μg mL^{-1} transferrin, 100 g mL^{-1} hydrocortisone, 50 μmol L^{-1} HEPES.

All cells were cultured under a humidified atmosphere at 37 °C and 5 % CO_2.

Cell migration inhibitory property by scratch wound-healing assay

HN22 cells were seeded into a 6-well plate (3.5×10^5 cells per well) and allowed to expand for 2 days until a confluent monolayer was formed. Three straight lines were

*Table I. Appearance and spectral data of compounds **1** and **2***

Characterization	5-Methoxy-3-(3-methyl-2,3-dihydroxybutyl)-psoralen (compound **1**)		5-Methoxy-3-(3-methyl-2,3-dihydroxybutyl)-psoralen diacetate (compound **2**)	
Appearance	White needles		Yellow amorphous solid	
UV λ_{max} (nm) (log ε)	221 (4.05), 249 (3.97), 260 (3.85), 269 (3.96), 314 (3.85)		221 (4.08), 249 (3.90), 261 (3.85), 269 (3.85), 313 (3.80)	
HR-ESI-MS	*m/z* 341.0989 $[M+Na]^+$ (calcd. for $C_{17}H_{18}O_6Na$ 341.1001) *m/z* 319.1185 $[M+H]^+$ (calcd. for $C_{17}H_{19}O_6$ 319.1181)		*m/z* 425.1211 $[M+Na]^+$ (calcd. for $C_{21}H_{22}O_8Na$ 425.1213) *m/z* 403.1382 $[M+H]^+$ (calcd. for $C_{21}H_{23}O_8$ 403.1393)	
^{1}H NMR data (300 MHz, $CDCl_3$)	Position	δ_H (ppm) (*J* in Hz)	Position	δ_H (ppm) (*J* in Hz)
	4	8.08, s, 1H	4	7.99, s, 1H
	8	7.12, s, 1H	8	7.13, s, 1H
	2′	7.58, d, (2.4), 1H	2′	7.59, d, (2.4), 1H
	3′	7.01, dd, (2.3, 0.7), 1H	3′	7.00, dd, (2.4, 0.4), 1H
	1″	2.87, dd (14.2, 1.1), 1H	1″	3.05, dd (14.5, 2.4), 1H
		2.57, dd (14.2, 10.1), 1H		2.70, dd (14.5, 10.4), 1H
	2″	3.71, dd (10.1, 1.5), 1H	2″	5.37, dd (10.3, 2.4), 1H
	4″	1.29, s, 3H	4″	1.58, s, 3H
	5″	1.33, s, 3H	5″	1.60, s, 3H
	5-OMe	4.26, s, 3H	5-OMe	4.26, s, 3H
			2″-OAc	2.01, s, 3H
			3″-OAc	1.99, s, 3H
^{13}C NMR data (75 MHz, $CDCl_3$)	Position	δ_C (ppm)	Position	δ_C (ppm)
	2	163.5	2	161.9
	3	122.6	3	121.4
	4	137.1	4	136.0
	4a	106.9	4a	106.8
	5	149.0	5	149.0
	6	112.8	6	112.9
	7	157.8	7	157.8
	8	93.5	8	93.8
	8a	151.8	8a	152.0
	2′	144.7	2′	144.7
	3′	105.0	3′	104.9
	1″	34.1	1″	30.9
	2″	77.3	2″	76.1
	3″	73.0	3″	82.3
	4″	23.9	4″	22.4
	5″	26.2	5″	22.5
	5-OMe	60.1	5-OMe	60.2
			2″-OAc	170.1 (C=O), 22.1 (CH_3)
			3″-OAc	170.2 (C=O), 20.8 (CH_3)

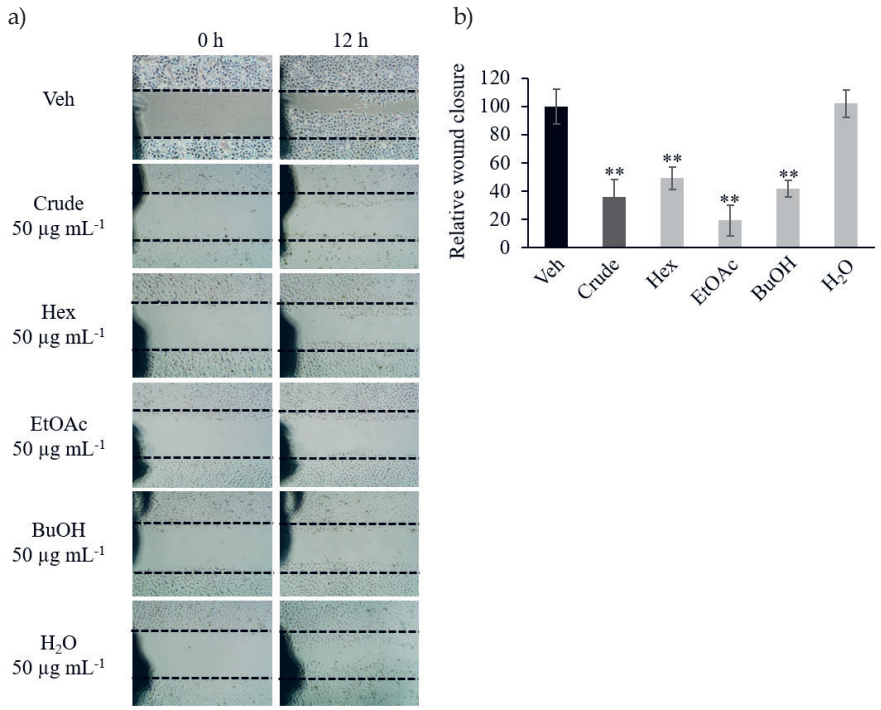


Fig. 2. Crude extract and polarity-based fraction of *D. foetida* inhibition of HN22 cancer cell lines migration in wound-healing assay. a) Representative image of wound area; b) relative wound closure. Data presented as mean ± SD, $n = 3$. Statistically significant difference *vs*. vehicle control (Veh): $^{**}p < 0.01$.

etched onto the culture surface with a P200 pipet tip. Detached cells were washed with phosphate-buffered saline (PBS). Culture media supplemented with FBS at reduced concentration (1 % FBS) and containing the crude extract or fractions at 50 μg mL^{-1} final concentration were added to each well. DMSO (0.5 %) was used as vehicle control. Five different locations of the wound area where pictures were to be taken were marked with a permanent pen. Pictures of the wound area at the same location were taken at 0 h and 12 h after treatment (Fig. 2a). The wound area was quantified by the ImageJ program (19). Results were displayed as a percentage of relative wound closure normalized to the vehicle control group (Fig. 2b).

MTT assay

MTT assay was employed to determine cell viability and performed according to an established protocol (20) with some modifications. Briefly, once the designated exposure time was reached, the stock solution of MTT was added into each well (1.25 mg mL^{-1} final concentration) and incubated for 4 h at 37 °C. Then, the culture medium was discarded, and 100 μL DMSO was added to each well. Absorbance at 550 nm was measured by UV-Vis VICTOR Nivo Multimode Microplate Reader (PerkinElmer, USA).

Table II. Cytotoxicity screening of D. foetida *whole plant crude ethanolic extract and polarity-based fractions*

Cell line	Cell viability inhibition (%)[a]									
	500 (μg mL^{-1})					50 (μg mL^{-1})				
	Crude	Hex	BuOH	EtOAc	H_2O	Crude	Hex	BuOH	EtOAc	H_2O
HaCaT	91.1 ± 1.11	95.1 ± 0.28	93.7 ± 0.40	88.4 ± 0.53	67.4 ± 1.46	36.3 ± 2.28	33.8 ± 7.67	24.9 ± 9.26	21.6 ± 9.39	1.5 ± 4.01
HCT116	95.8 ± 0.16	97.6 ± 0.13	96.1 ± 0.13	97.0 ± 0.18	75.8 ± 1.99	47.1 ± 3.92	95.9 ± 1.14	91.7 ± 0.40	83.4 ± 2.40	11.2 ± 3.25
HT29	94.7 ± 0.66	97.7 ± 0.26	94.3 ± 0.49	93.9 ± 0.29	78.4 ± 0.70	30.3 ± 2.78	94.0 ± 0.78	82.5 ± 1.22	52.3 ± 1.71	9.7 ± 6.27
MCF7	90.2 ± 0.81	94.4 ± 0.93	85.0 ± 0.42	91.1 ± 0.17	88.4 ± 0.52	2.8 ± 2.78	18.4 ± 1.79	12.0 ± 0.40	5.5 ± 1.10	1.0 ± 0.86
MDA-MB-231	97.4 ± 0.03	98.6 ± 0.09	95.6 ± 0.32	94.4 ± 0.59	78.7 ± 0.61	3.9 ± 5.72	31.9 ± 3.26	57.3 ± 1.07	6.3 ± 3.83	–6.6 ± 2.50
HepG2	65.6 ± 1.05	95.1 ± 0.60	91.0 ± 0.41	85.4 ± 3.08	39.8 ± 2.29	–25.9 ± 5.25	–3.0 ± 0.65	–4.5 ± 2.99	–31.3 ± 8.31	–1.5 ± 1.24
HN22	96.1 ± 0.10	97.8 ± 0.17	72.4 ± 1.00	91.6 ± 0.34	40.7 ± 0.40	30.0 ± 6.25	41.0 ± 1.82	50.0 ± 1.64	21.7 ± 1.68	1.8 ± 0.94

[a] Mean ± SD, $n = 3$.

Cytotoxicity tests

Cytotoxicity tests were performed in a 96-well plate. All cells were seeded at 8×10^3 cells per well and allowed to attach overnight. Crude extract and fractions were first screened for cytotoxic activity at two concentrations, *i.e.*, 500 and 50 μg mL^{-1}, against various cancer cell lines including HCT116, HT29, MCF7, MDA-MB-231, HepG2, and HN22. The non-cancerous cell line HaCaT was used as a normal cell control. DMSO was used as vehicle control and maintained at 0.5 % (*V*/*V*) final concentration in a cell culture medium for all test conditions. Cells were exposed to the test agents for 72 h. Then, cell viability was measured as described in the MTT assay. All experiments were done in triplicate. The percentage of cell viability inhibition was calculated for cells treated with 500 and 50 μg mL^{-1} of crude extract and fractions and presented in Table II).

To further validate the cytotoxic effect observed in the screening test, HCT116 and HT29 lines were treated with crude extract or fractions at 500, 100, 20, 4, 0.8, 0.16 μg mL^{-1} final concentration. DMSO was used as vehicle control and maintained at 0.5 % (*V*/*V*) final concentration in a cell culture medium for all test conditions. Iri (100 μmol L^{-1} final concentration) was used as a positive control. Cells were exposed to the test agents for 72 h. Then, cell viability was measured as described in the MTT assay. All experiments were done in triplicate. Data were presented as the percentage of cell viability relative to the vehicle control (Fig. 3).

To study the cytotoxic activity of the isolated compounds **1** and **2**, cancer cell lines HCT116, HT29, MDA-MB-231, and HN22 were treated with compound **1** or **2** at varying concentrations (250–0.08 μmol L^{-1}) (Fig. 4). The non-cancerous cell line HaCaT was used as a normal cell control. DMSO-HPBCD was used as vehicle control and maintained

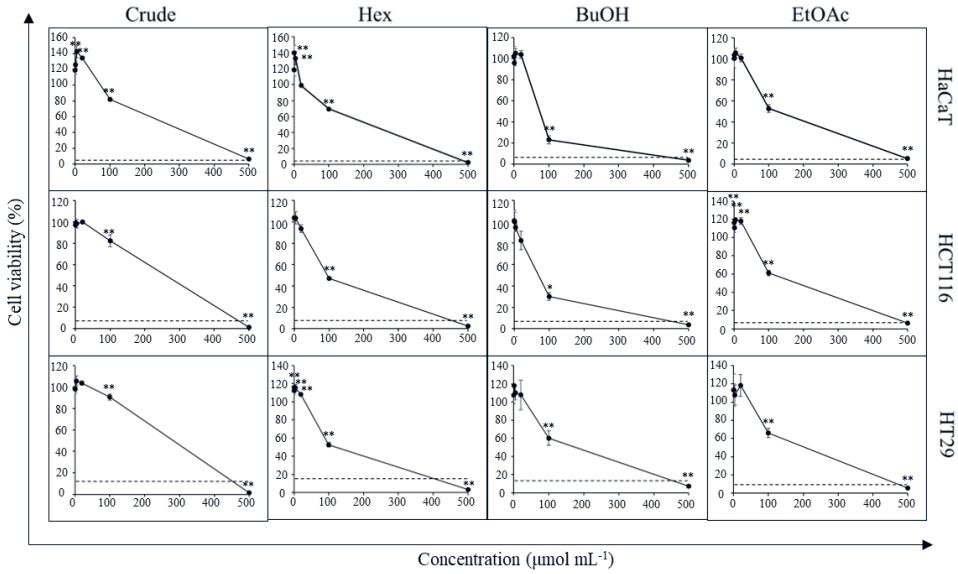


Fig. 3. Cytotoxic activity of *D. foetida* extracts. Cell viability of HCT116, HT29 and HaCaT cells cells cells treated with 0.16–500 μg mL^{-1} of crude extract and polarity-based fractions of *D. foetida*. Iri (100 μmol L^{-1}) was used as a positive control (dash line). Data presented as mean ± SD, $n = 3$. Statistically significant difference *vs*. vehicle control: $^{**}p < 0.01$, $^{*}p < 0.05$.

at 0.5 % (*V/V*) final concentration for all test conditions. Iri (100 μmol L^{-1} final concentration) was used as a positive control. Cells were exposed to the test agents for 72 h. Cell viability was then measured as described in the MTT assay. All experiments were done in triplicate. Data were presented as the percentage of cell viability relative to vehicle control.

IC_{50} was calculated using the non-linear regression equation log (inhibitor) *vs*. normalized response-variable slope (21). The IC_{50} value of compound **2** is given in Fig. 5.

*Cytotoxic activity of compound **2** in combination with Iri*

HCT116 cells were seeded as described above. First, cells were treated with a fixed concentration of Iri at 5 μmol L^{-1} while the concentration of compound **2** was varied from 50–250 μmol L^{-1}. Subsequently, cells were treated with a fixed Iri:**2** concentration ratio of 1:40 (Iri 0.625–5 μmol L^{-1} and compound **2** 25–200 μmol L^{-1}) (Fig. 6).

To assess the cytotoxicity of compound **2** and Iri combination against normal cells, FHC cells were treated with the combination Iri:**2** at 1:40 (Iri 2.5 μmol L^{-1} + compound **2** 100 μmol L^{-1}), or each individual agent at the same concentration for 72 h (Fig. 7).

In the both above cases, vehicle control, exposure time, cell viability determination, and data presentation were as described in cytotoxicity tests of individual compounds.

Cell viability data obtained from the combination experiments was analyzed *via* CompuSyn software to calculate the combination index (CI) and evaluate the pharmacological

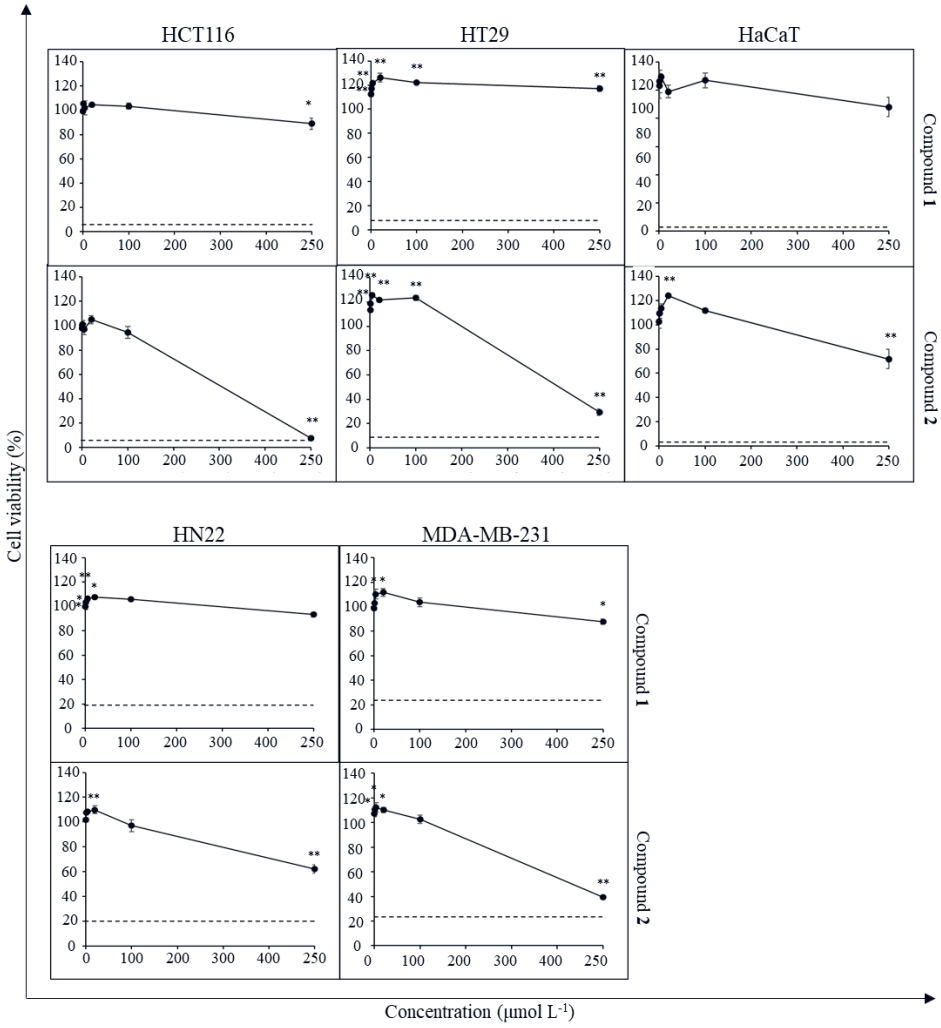


Fig. 4. Cytotoxic activity of compounds **1** and **2** against cancer cell lines and HaCaT cells. Dash line represents the viability of cells (%) treated with 100 μmol L^{-1} Iri. Data presented as mean ± SD, $n = 3$. Statistically significant difference *vs*. vehicle control: $^{**}p < 0.01$, $^{*}p < 0.05$.

interaction, *i.e.*, antagonistic (CI >1), additive (CI =1), or synergistic relationships (CI <1) using Chou-Talalay method (22, 23). Lastly, dose reduction index (DRI) which is a fold reduction of drug dose in a single treatment relative to its dose in combination treatment required to reach the same inhibitory effect was calculated; DRI >1 favors dose reduction, whereas DRI <1 disfavors dose reduction. Additionally, the prediction of the dose required to achieve 50–90 % inhibition and types of interaction were also calculated by CompuSyn software (Table III, Fig. 8).

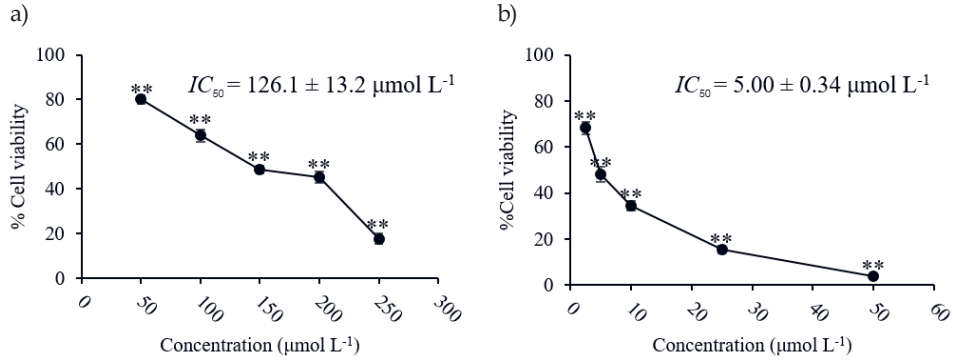


Fig. 5. Cytotoxic activity and IC_{50} of: a) compound **2** and b) Iri against HCT116 cell line. Data presented as mean ± SD, $n = 3$. Statistically significant difference *vs.* vehicle control: $^{**}p < 0.01$.

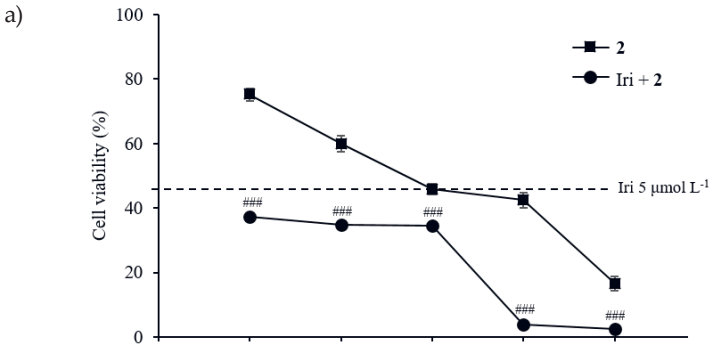
Apoptosis analysis using fluorescence microscopy

HCT116 cells were seeded into a 96-well plate (8×10^3 cells per well) and allowed to attach overnight. Cells were then treated with Iri (2.5 μmol L^{-1}), compound **2** (100 μmol L^{-1}), or the combination of both (2.5 μmol L^{-1} Iri + 100 μmol L^{-1} compound **2**) for 24 h. DMSO-HPBCD was used as vehicle control and maintained at 0.5 % (*V*/*V*) for all conditions. Afterwards, cells were stained with Hoechst 33342 (5 mg mL^{-1}) and SYTOX® Green (0.1 μmol L^{-1}) in PBS for 15 min while protected from light. Images from three different microscopic fields were then taken using an inverted fluorescent microscope (Eclipse TE 2000-U, Nikon, Japan), 10× magnification under DAPI filter (358 nm excitation/461 nm emission) for Hoechst 33342, Blue Excitation (B-2A) filter (450–490 nm excitation/515 nm emission) for SYTOX® Green and bright-field (Fig. 7a). In each microscopic field, all cell nuclei stained with Hoechst 33342 (blue fluorescence) were counted for total cell number. The number of condensed nuclei showing bright blue fluorescence stained with Hoechst 33342 was counted for apoptotic cells. The number of leaky cells showing green fluorescence from SYTOX® Green staining was counted for dead cells. Bar graphs represent the percentage of apoptotic cells, dead cells and total dead cells (apoptotic cells + dead cells) normalized to the total cell number in each microscopic field (Fig. 7b).

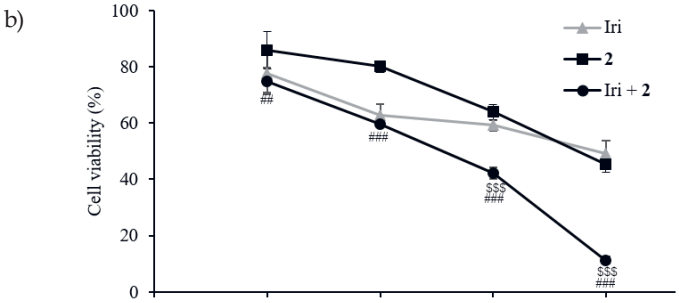
Data analysis

All data were expressed as mean ± standard deviations (SD). One-way ANOVA followed by Tukey HSD *post hoc* test was performed to determine the statistical significance of cytotoxic activity and anti-migratory activity of extracts, compounds **1** and **2,** and Iri when compared to vehicle control. Two-way ANOVA followed by Sidak's test was used to determine the statistical significance of cytotoxic activity and percentage of apoptotic and dead cells for compound **2**, Iri, and Iri+**2** combination. p-value < 0.05 was considered statistically significant.

GraphPad Prism software version 7 was used for all statistical analysis and IC_{50} calculations.



Compound **2** (μmol L^{-1})	50	100	150	200	250
Iri:2 ratio	1:10	1:20	1:30	1:40	1:50
CI	0.94	1.05	1.24	0.15	0.10
Interpretation	nearly additive (±)	nearly additive (±)	moderate antagonism (--)	strong synergism (++++)	strong synergism (++++)
DRI Iri	1.39	1.51	1.52	12.43	19.23
DRI compound **2**	4.63	2.55	1.72	14.34	19.94



Iri (μmol L^{-1})	0.625	1.25	2.5	5
Compound **2** (μmol L^{-1})	25	50	100	200
Iri:2 ratio	1:40	1:40	1:40	1:40
CI	1.43	1.07	0.86	0.24
Interpretation	moderate antagonism (--)	nearly additive (±)	slight synergism (+)	synergism (+++)
DRI Iri	1.07	1.80	3.03	30.56
DRI compound **2**	2.02	1.96	1.90	4.91

Fig. 6. Synergistic anticancer activity between compound **2** and Iri in HCT116 cells. a) Cell viability of HCT116 exposed to Iri (fixed Iri concentration at 5 μmol L^{-1}), compound **2** (50–250 μmol L^{-1}), or the combination of Iri and compound **2** (Iri+**2**). b) Cell viability of HCT116 exposed to compound **2** and Iri (fixed Iri:**2** molar ratio at 1:40). Data presented as mean ± SD, $n = 3$. Statistically significant difference: *vs.* compound **2** monotherapy at the same concentration: $^{\#\#}p < 0.01$, $^{\#\#\#}p < 0.001$; *vs.* Iri monotherapy at the same concentration: $^{\$\$\$}p < 0.001$.

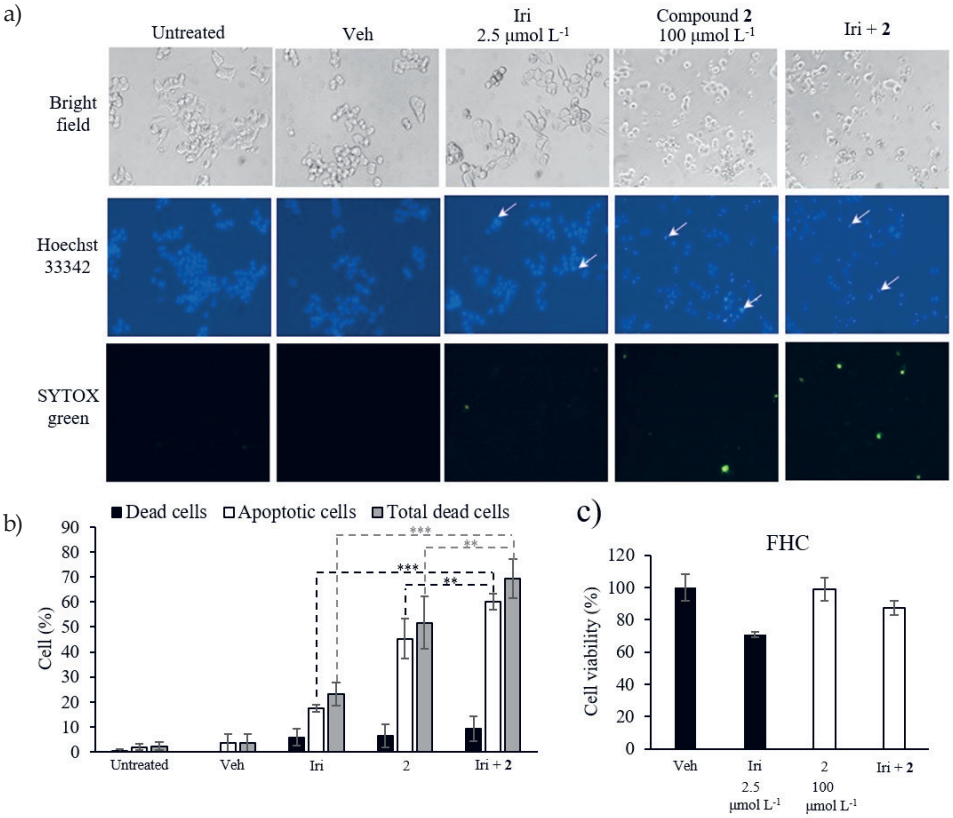


Fig. 7. Apoptosis analysis by Hoechst 33342 and SYTOX® Green double staining. a) Representative images from an inverted fluorescent microscope. [Apoptotic cells appear with bright blue fluorescence of Hoechst 33342 staining (white arrows); dead cells show green fluorescence of SYTOX® Green staining]; b) percentage of apoptotic and dead cells; c) cytotoxicity of Iri, compound **2** and Iri+**2** against FHC cells. Data presented as mean ± SD, $n = 3$. Statistically significant difference *vs*. respective monotherapy: ***$p < 0.001$, **$p < 0.01$.

RESULTS AND DISCUSSION

Isolation of and identification of pure compounds

Given the promising cytotoxic and anti-migratory activity of the EtOAc fraction, it was selected for further purification. Chromatographic separation of the EtOAc extract of *D. foetida* provided two known linear furanocoumarins, *i.e.*, 5-methoxy-3-(3-methyl-2,3--dihydroxybutyl)-psoralen (**1**) and 5-methoxy-3-(3-methyl-2,3-dihydroxybutyl)-psoralen diacetate (**2**) (Fig. 1). The chemical structures of the isolated compounds were characterized on the basis of the spectroscopic data (UV, NMR and MS, Table I and supplementary data, Figs. S1-S6).

Compound **1** was obtained as white needles from ethanol. Its molecular formula was determined to be $C_{17}H_{18}O_6$ by HRESIMS as *m/z* 341.0989 $[M+Na]^+$ (calcd. for $C_{17}H_{18}O_6Na$ 341.1001) and 319.1185 $[M+H]^+$ (calcd. for $C_{17}H_{19}O_6$ 319.1181). The ^{1}H- and ^{13}C NMR spectra of compound **1** were identical to 5-methoxy-3-(3-methyl-2,3-dihydroxybutyl)-psoralen, a component found in the other species of *Dorstenia* namely *D. gigas* (24) and *D. turbinata* (25). However, to the best of our knowledge, this compound is reported for the first time in *D. foetida*.

Compound **2** was isolated as a yellow amorphous solid. The molecular formula of compound **2** was established as $C_{21}H_{22}O_8$ derived from HRESIMS of its $[M+Na]^+$ peak at *m/z* 425.1211 $[M+Na]^+$ (calcd. for $C_{21}H_{22}O_8Na$ 425.1213) and $[M+H]^+$ peak at *m/z* 403.1382 (calcd. for $C_{21}H_{23}O_8$ 403.1393). The NMR data of compound **2** were similar to those of compound **1** except for the presence of two acetate groups in compound **2**. The acetate signals were clearly indicated by the corresponding ^{13}C NMR signals at d_C 170.2, 170.1, 22.1, and 20.8 ppm as well as the proton resonances at d_H 2.01 (3H, s) and 1.99 (3H, s) ppm. The remaining NMR data of compound **2** were identical to the structure of 5-methoxy-3-(3-methyl-2,3-dihydroxybutyl)-psoralen diacetate, which was previously isolated from the same plant (18).

Extraction, fractionation, and preliminary screening of anticancer activity

First, we sought to confirm whether the *D. foetida* whole plant possessed any anticancer activity or not. In this regard, crude ethanolic extract and polarity-based fractions, *i.e.*, Hex, BuOH, EtOAc, and H_2O, were screened for cytotoxic activity against various cancer cell lines while using HaCaT cell line as a representative of non-cancerous cells. The results revealed that the crude ethanolic extract and Hex, BuOH, EtOAc, and H_2O fractions were cytotoxic against most cell lines at high concentrations (500 μg mL^{-1}) (Table II). Ten-fold lower concentration (50 μg mL^{-1}) revealed that crude extract exhibited moderate cytotoxic activity (25–75 % inhibition) against HCT116, HT29, and HN22 cells and weak to no inhibition (< 25 % inhibition) against MCF7, MDA-MB-231 and HepG2 cells, whereas negligible cytotoxic activity was observed for H_2O fraction. Hex, BuOH, and EtOAc fractions demonstrated a strong cytotoxic activity (≥ 75 % inhibition) against many cancer cell lines, especially HCT116 and HT29. Moreover, the cytotoxic activities against colorectal cancer cell lines of these fractions were increased compared to that of the crude extract. Notably, the cytotoxic activity of Hex, BuOH, and EtOAc fractions was more potent against HCT116 and HT29 cancer cells compared to non-cancerous cells HaCaT.

The cytotoxic effect of Hex, BuOH, and EtOAc fractions was further examined at more concentration intervals. Indeed, the cytotoxicity against colorectal cancer cell lines of all fractions was recapitulated (Fig. 3). However, the BuOH fraction appeared to be slightly more toxic against the normal cell HaCaT than HCT116 and HT29 cells. Additionally, while the cytotoxic activity at 100 and 500 μg mL^{-1} of Hex and EtOAc fraction was comparable, growth-promotion activity was detected in Hex fraction at low concentration (< 4 μg mL^{-1}).

Aside from cytotoxic activity, crude ethanolic extract and polarity-based fractions of *D. foetida* were also screened for cell migration inhibitory activity. Using the wound-healing assay, cell migration inhibitory activity was detected in crude extract (Fig. 2). While such activity was lost in the H_2O fraction, cell migration inhibition activity was retained in Hex, BuOH, and EtOAc fractions. Among these fractions, EtOAc appeared to exhibit a stronger cell migration inhibition activity compared to that of the crude extract, although such a difference was not statistically significant.

Cytotoxicity of isolated compounds

The cytotoxic activity of compounds **1** and **2** was then investigated in cancer cell lines (Fig. 4). The results revealed that compound **2** exhibited cytotoxic activity against HN22, MDA-MB-231, HCT116, and HT29 cells, although such activity was detected at a high concentration (250 μmol L^{-1}) and no concentration-dependence was observed at the concentrations tested. In line with the previous screening studies, the cytotoxic activity of compound **2** was more prominent against colorectal cancer cell lines. Notably, although the two compounds share the same core structure, compound **1** exhibited negligible cytotoxic activity.

Given that compound **2** appeared to have the strongest inhibitory effect against HCT116 cells, we next sought to explore whether this compound can be used in concert with an established anticancer agent, irinotecan (Iri), to potentiate its effect. Irinotecan, an inhibitor of topoisomerase I, routinely prescribed in colorectal cancer, was selected as a model for anticancer agents. Half-maximal inhibitory concentrations (IC_{50}) of compound **2** (126.1 ± 13.2 μmol L^{-1}) and Iri (5.0 ± 0.34 μmol L^{-1}) were first determined in HCT116 cells (Fig. 5).

Next, the pharmacological interaction, *i.e.*, antagonistic, additive, or synergistic effect, between compound **2** and Iri was investigated. First, Iri and **2** were combined at various molar ratios (Iri:**2** = 1:10 to 1:50) with the varying concentration of compound **2** (50–250 μmol L^{-1}) while the concentration of Iri was fixed at 5 μmol L^{-1} (Fig. 6a). The Iri:**2** ratios of 1:40 and 1:50 revealed a strong synergistic interaction with low combination index (CI) values (0.17 and 0.12, resp.). Such effect was diminished at the lower ratios, *i.e.*, 1:10, 1:20, and 1:30, suggesting that these two agents likely exhibit synergy only at high concentration of compound **2**.

Since a sharp decrease in cell viability was detected at a 1:40 Iri:**2** ratio compared to monotherapy by compound **2** or Iri at the same concentrations (Fig. 6a), this ratio was selected for further investigation. In this experiment, HCT116 cells were treated with 1:40 Iri:**2** ratio (Fig. 6b), with varying concentrations of compound **2** (25–200 μmol L^{-1}) and Iri (0.625–5 μmol L^{-1}). In line with the previous observation, the synergism of compound **2** and Iri was more prominent at high concentrations (> 2.5 μmol L^{-1} for Iri and > 100 μmol L^{-1} for compound **2**).

To further explore the interplay between compound **2** and Iri, the cell viability values for 1:40 Iri:**2** ratio treatments were converted to a percentage of cell viability inhibition and

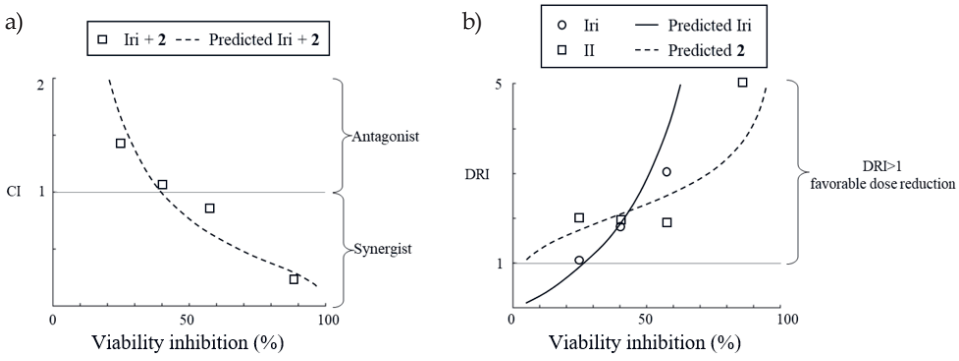


Fig. 8. a) The combination index plot; b) the dose reduction index plot with viability inhibition simulated by CompuSyn software using the cell viability data from the Iri:**2** = 1:40 combination experiment.

Table III. Simulation data obtained from CompuSyn software[a]

Viability inhibition HCT116 cells (%)	Predicted dose depicted as Iri:**2** 1:40 combination/single agent		Predicted combination index (CI)	Grade of CI	Interpretation	Dose reduction index (DRI)	
	Iri (μmol L^{-1})	Compd. **2** (μmol L^{-1})				Predicted DRI of Iri	Predicted DRI of compd. **2**
50	1.55/4.48	60.64/141.29	0.78	++	Moderate synergism	2.89	2.33
60	2.05/9.04	79.95/207.07	0.61	+++	Synergism	4.41	2.59
70	2.77/19.36	108.05/313.35	0.49	+++	Synergism	6.99	2.90
80	4.00/49.00	156.04/519.61	0.38	+++	Synergism	12.25	3.33
90	6.96/198.29	271.25/1,117.55	0.27	+++	Synergism	28.49	4.12

analyzed by CompuSyn software (Combosyn, Inc., USA) to calculate CI and DRI (the ratio of dose of an agent required to reach a particular inhibitory effect when used as monotherapy to the dose of the same agent to achieve the same effect when used in the combination) across the range of cell viability inhibition effects (Fig. 8). The analysis revealed that the CI value of the combination ratio Iri:**2** of 1:40 decreased with increasing concentration of the two agents (Fig. 8a). Moreover, DRI analysis revealed that the combination at this ratio conveyed benefits in dose reduction (DRI > 1) over a broad range of concentrations (Fig. 8b).

Next, the cytotoxic activity data of the 1:40 Iri:**2** combination was analyzed to predict the dose of each agent, when used as monotherapy and as a combined treatment, to achieve a 50–90 % inhibitory effect (Table III). The simulation indicated that the two agents exhibited synergistic activity throughout this range of inhibition effects, indicating dose-reduction of both agents. Notably, a dose-reduction of ~28 fold and ~4 fold was predicted for Iri and compound **2**, resp., when applied in combination in order to achieve 90 % viability inhibition compared to when applied individually (predicted IC_{90} concentration of Iri and compound **2**:6.96 μmol L^{-1} in combination *vs.* 198.29 μmol L^{-1} as monotherapy, 271.25 μmol L^{-1} in combination *vs.* 1117.55 μmol L^{-1} as monotherapy, resp.). Together, our findings suggest that combining Iri and compound **2** could potentiate cytotoxic activity against HCT116 cells through synergism and allow dose reduction of each drug.

Given the promising cytotoxicity result of the combination ratio Iri:**2** 1:40, this combination ratio was selected for further analysis through another complementary assay, *i.e.*, the determination of cells undergoing apoptosis using a fluorescent imaging technique. In this study, apoptotic cells that exhibited characteristic nuclear condensation and fragmentation

appeared bright blue with Hoechst 33342 staining (Fig. 7a, arrowed) while dead cells exhibiting a compromised cell membrane integrity were stained green with SYTOX® Green dye. The ratio of cells exhibiting bright blue nucleus compared to total cell number (total nuclei) in the same microscopic field thus reflected the percentage of apoptotic cells, while the ratio of cells stained green with SYTOX® Green compared to total cell number in the same field indicated the percentage of dead cells. The sum of apoptotic cells and dead cells was thus interpreted as total dead cells. Indeed, the result revealed that the percentage of apoptotic and dead cells was markedly increased in HCT116 cells treated with the combination of Iri and compound **2** at a 1:40 ratio (Fig. 7b, supplementary Table SI) compared to cells treated with each agent individually at the same concentration, supporting the synergistic relationship. Lastly, to further explore the safety threshold of Iri:**2** at 1:40 (Iri 2.5 μmol L^{-1} + compound **2** 100 μmol L^{-1}), the cytotoxic activity of this combination, along with that of each individual agent, was investigated using fetal colonic epithelial cell line FHC. The result revealed that the combination elicited mild cytotoxic activity (% inhibition ~13 %) against non-cancerous colonic epithelial cells (Fig. 7c) compared to ~60 % cell viability inhibition in HCT116 cells (Fig. 6b), suggesting the existence of a potential therapeutic window of the combination. Indeed, no anticancer compound is completely non-toxic; the challenge thus lies in the characterization of the therapeutic window, as well as identifying the specific cancer types susceptible to the treatment.

Although the isolation of compound **2** has been reported, data regarding its biological activity remains largely elusive. Indeed, psoralen, the parental structure of compound **2**, and its derivatives have been demonstrated to exhibit a wide range of biological activities including anti-osteoporotic, anti-inflammatory, insecticidal, antibacterial, antifungal, and cytotoxic (26, 27). Our report thus revealed that compound **2** harbored potential cytotoxic activity, particularly against colorectal cancer cell lines. Additionally, our results served as a proof of concept that compound **2** could be used synergistically with the anticancer agent Iri against colorectal cancer in combination therapy, enabling a dose reduction of each agent.

Like other cancer types, colorectal cancer exhibited inter-personal variability which complicates treatment selection. Indeed, colorectal cancer has been classified into four distinct consensus molecular subtypes (CMSs) with genetic abnormalities specific for each group (28, 29). Consequently, the same molecular criteria have been used to classify established colorectal cancer cell lines (30). Each CMS subclass has been shown to exhibit distinct drug response profiles both *in vitro* and in clinical settings (29, 31, 32). Therefore, it may be worthwhile to investigate the effect of compound **2**, when used by itself and in combination with other anticancer agents, using established cancer cell lines representing specific subclasses of colorectal cancer.

CONCLUSIONS

This report describes the isolation and identification of furanocoumarin compounds, 5-methoxy-3-(3-methyl-2,3-dihydroxybutyl)-psoralen (**1**) and 5-methoxy-3-(3-methyl-2,3-dihydroxybutyl)-psoralen diacetate (**2**) from ethyl acetate fraction of the whole plant of *D. foetida*, and the investigation of their anticancer properties. Results revealed that compound **2** exhibited cytotoxic activity against diverse cancer cell types, especially colorectal cancer. Further analysis of the interplay between compound **2** and the model drug irino-

tecan (Iri) was investigated in HCT116 in a series of combination treatments. It was found that a combined treatment of compound **2** and Iri elicited a synergistic effect at certain ratios and concentrations. This synergism was further supported by the increase in the percentage of apoptotic cells in HCT116 treated with the combination at 1:40 Iri:**2** molar ratio compared to that of the cells treated with each individual agent at the same concentration. Altogether, our results identified compound **2** as a potential anticancer agent of plant origin which can be used synergistically with Iri. Our results thus warranted further research to assess the potential of this synergism for colorectal cancer treatment and to fine-tune the concentration of both agents, exploiting the therapeutic window, to maximize anticancer activity while minimizing the adverse effects.

Supplementary materials are available upon request.

Acronyms, abbreviations, symbols. – BuOH – *n*-butanol, CI – combination index, CMS – consensus molecular subtype, DMEM – Dulbecco's modified Eagle's medium, DMSO – dimethyl sulfoxide, DMSO-HPBCD – 30 % (*m*/*V*) hydroxypropyl-β-cyclodextrin, DRI – dose reduction index, FBS – fetal bovine serum, EtOAc – ethyl acetate, hEGF – human epithelial growth factor, Hex – *n*-hexane, HRMS – high-resolution mass spectra, IC_{50} – half-maximal inhibitory concentration, Iri – irinotecan, MTT – 3-(4,5-dimethylthiazol-2-yl)-2,5-diphenyltetrazoliumbromide, NEAA – non-essential amino acids, Pen/Strep – penicillin/streptomycin, TMS – tetramethylsilane.

Acknowledgements. – We thank professors Praneet Opanasopit for providing HCT116, HT29, MCT7, MDA-MB-231, HepG2, HN22 cell lines and HPBCD, and Veerawat Teeranachaidekul for HaCaT cell line, Nattiya Kapol for Iri, Purin Charoensuksai and Worrakanya Narakornwit for botanical identification and John Tigue for English language editing and critical reading of the manuscript. We thank the Faculty of Pharmacy, Silpakorn University, for its research facilities and instruments.

Conflict of interest. – The authors declare no conflict of interest.

Funding – This publication is a part of the research project "Anticancer activities of *Dorstenia foetida* and activity augmentation through a combination treatment with siRNA-mediated gene targeting" financially supported by Thailand Science Research and Innovation (TSRI) National Science Research and Innovation Fund (NSRF) Fiscal Year 2565BE (Grant number 65A114000042).

Authors contributions. – Conceptualization, P.C., S.P. and K.R.; methodology, P.C., S.P. and K.R.; analysis P.C., P.W., S.P. and K.R.; investigation, W.J. and R.S.; writing, original draft preparation, P.C., P.W., S.P. and K.R.; writing, review and editing, P.C., P.W., S.P. and K.R. All authors have read and agreed to the published version of the manuscript.

REFERENCES

1. D. Hanahan and R. A. Weinberg, Hallmarks of cancer: The next generation, *Cell* **144**(5) 646–674; https://doi.org/10.1016/j.cell.2011.02.013
2. R. L. Siegel, K. D. Miller and A. Jemal, Cancer statistics, 2016, *CA Cancer J. Clin*. **66**(1) (2016) 7–30; https://doi.org/10.3322/caac.21332
3. M. Vanneman and G. Dranoff, Combining immunotherapy and targeted therapies in cancer treatment, *Nat. Rev. Cancer* **12**(4) (2012) 237–251; https://doi.org/10.1038/nrc3237
4. A. Pathak, S. Tanwar, V. Kumar and B. D. Banarjee, Present and future prospect of small molecule & related targeted therapy against human cancer, *Vivechan Int. J. Res.* **9**(1) (2018) 36–49.
5. F. A. Fisusi and E. O. Akala, Drug combinations in breast cancer therapy, *Pharm. Nanotechnol*. **7**(1) (2019) 3–23; https://doi.org/10.2174/2211738507666190122111224

6. B. B. Mishra and V. K. Tiwari, Natural products: an evolving role in future drug discovery, *Eur. J. Med. Chem.* **46**(10) (2011) 4769–4807; https://doi.org/10.1016/j.ejmech.2011.07.057
7. G. M. Cragg and D. J. Newman, Plants as a source of anti-cancer agents, *J. Ethnopharmacol.* **100**(1–2) (2005) 72–79; https://doi.org/10.1016/j.jep.2005.05.011
8. F. M. de Man, A. K. L. Goey, R. H. N. van Schaik, R. H. J. Mathijssen and S. Bins, Individualization of irinotecan treatment: A review of pharmacokinetics, pharmacodynamics, and pharmacogenetics, *Clin. Pharmacokinet.* **57**(10) (2018) 1229–1254; https://doi.org/10.1007/s40262-018-0644-7
9. A. B. Benson, A. P. Venook, M. M. Al-Hawary, M. A. Arain, Yi-J. Chen, K. K. Ciombor, S. Cohen, H. S. Cooper, D. Deming, L. Farkas, I. Garrido-Laguna, J. L. Grem, A. Gunn, J. R. Hecht, S. Hoffe, J. Hubbard, S. Hunt, K. L. Johung, N. Kirilcuk, S. Krishnamurthi, W. A. Messersmith, J. Meyerhardt, E. D. Miller, M. F. Mulcahy, S. Nurkin, M. J. Overman, A. Parikh, H. Patel, K. Pedersen, L. Saltz, C. Schneider, D. Shibata, J. M. Skibber, C. T. Sofocleous, E. M. Stoffel, E. Stotsky-Himelfarb, C. G. Willett, K. M. Gregory and L. A. Gurski, Colon cancer, Version 2.2021, NCCN Clinical Practice Guidelines in Oncology, *J. Nat. Compreh. Cancer Network* **19**(3) (2021) 329–359; https://doi.org/10.6004/jnccn.2021.0012
10. A. J. Alonso-Castro, M. L. Villarreal, L. A. Salazar-Olivo, M. Gomez-Sanchez, F. Dominguez and A. Garcia-Carranca, Mexican medicinal plants used for cancer treatment: pharmacological, phytochemical and ethnobotanical studies, *J. Ethnopharmacol.* **133**(3) (2011) 945–972; https://doi.org/10.1016/j.jep.2010.11.055
11. N. F. Bussa and A. Belayneh, Traditional medicinal plants used to treat cancer, tumors and inflammatory ailments in Harari Region, Eastern Ethiopia, *South Afr. J. Bot.* **122** (2019) 360–368; https://doi.org/https://doi.org/10.1016/j.sajb.2019.03.025
12. T. Teklehaymanot and M. Giday, Ethnobotanical study of medicinal plants used by people in Zegie Peninsula, Northwestern Ethiopia, *J. Ethnobiol. Ethnomed.* **3** (2007) Article ID 12 (11 pages); https://doi.org/10.1186/1746-4269-3-12
13. T. Teklehaymanot, Ethnobotanical study of knowledge and medicinal plants used by the people in Dek Island in Ethiopia, *J. Ethnopharmacol.* **124**(1) (2009) 69–78; https://doi.org/10.1016/j.jep.2009.04.005
14. V. Kuete, B. Krusche, M. Youns, I. Voukeng, A. G. Fankam, S. Tankeo, S. Lacmata and T. Efferth, Cytotoxicity of some Cameroonian spices and selected medicinal plant extracts, *J. Ethnopharmacol.* **134**(3) (2011) 803–812; https://doi.org/10.1016/j.jep.2011.01.035
15. F. A. Adem, V. Kuete, A. T. Mbaveng, M. Heydenreich, A. Ndakala, B. Irungu, T. Efferth and A. Yenesew, Cytotoxic benzylbenzofuran derivatives from *Dorstenia kameruniana*, *Fitoterapia* **128** (2018) 26–30; https://doi.org/10.1016/j.fitote.2018.04.019
16 T. Uchiyama, S. Hara, M. Makino and Y. Fujimoto, seco-Adianane-type triterpenoids from *Dorstenia brasiliensis* (Moraceae), *Phytochemistry* **60**(8) (2002) 761–764.
17. V. Kuete, A. T. Mbaveng, M. Zeino, B. Ngameni, G. D. Kapche, S. F. Kouam, B. T. Ngadjui and T. Efferth, Cytotoxicity of two naturally occurring flavonoids (dorsmanin F and poinsettifolin B) towards multi-factorial drug-resistant cancer cells, *Phytomedicine* **22**(7–8) (2015) 737–743; https://doi.org/10.1016/j.phymed.2015.04.007
18. R. Heinke, K. Franke, A. Porzel, L. A. Wessjohann, N. A. Ali and J. Schmidt, Furanocoumarins from *Dorstenia foetida*, *Phytochemistry* **72**(9) (2011) 929–934; https://doi.org/10.1016/j.phytochem.2011.03.008
19. C. A. Schneider, W. S. Rasband and K. W. Eliceiri, NIH Image to ImageJ: 25 years of image analysis, *Nature Meth.* **9**(7) (2012) 671–675; https://doi.org/10.1038/nmeth.2089
20. P. Kumar, A. Nagarajan and P. D. Uchil, Analysis of cell viability by the MTT assay, *Cold Spring Harbor Protoc.* **2018**(6) (2018) 469–471; https://doi.org/10.1101/pdb.prot095505
21. S. W. Jarantow, E. D. Pisors and M. L. Chiu, Introduction to the use of linear and nonlinear regression analysis in quantitative biological assays, *Curr. Prot.* **3**(6) (2023) e801; https://doi.org/https://doi.org/10.1002/cpz1.801

22. I. V. Bijnsdorp, E. Giovannetti and G. J. Peters, Analysis of drug interactions, *Meth. Mol. Biol.* **731** (2011) 421–434; https://doi.org/10.1007/978-1-61779-080-5_34

23. T. C. Chou, Drug combination studies and their synergy quantification using the Chou-Talalay method, *Cancer Res.* **70**(2) (2010) 440–446; https://doi.org/10.1158/0008-5472.Can-09-1947

24. K. Franke, A. Porzel, M. Masaoud, G. Adam and J. Schmidt, Furanocoumarins from *Dorstenia gigas*, *Phytochemistry* **56**(6) (2001) 611–621; https://doi.org/10.1016/s0031-9422(00)00419-2

25. B. Ngameni, V. Kuete, I. K. Simo, A. T. Mbaveng, P. K. Awoussong, R. Patnam, R. Roy and B. T. Ngadjui, Antibacterial and antifungal activities of the crude extract and compounds from *Dorstenia turbinata* (Moraceae), *South Afr. J. Bot.* **75**(2) (2009) 256–261; https://doi.org/https://doi.org/10.1016/j.sajb.2008.11.006

26. J. Jamalis, F. S. M. Yusof, S. Chander, R. A. Wahab, P. B. D, M. Sankaranarayanan, F. Almalki and T. B. Hadda, Psoralen derivatives: Recent advances of synthetic strategy and pharmacological properties, *Antiinflamm. Antiallergy Agents Med. Chem.* **19**(3) (2020) 222–239; https://doi.org/10.2174/1871523018666190625170802

27. Y. Ren, X. Song, Lu Tan, C. Guo, M. Wang, H. Liu, Z. Cao, Y. Li and C. Peng, A review of the pharmacological properties of psoralen, *Front. Pharmacol.* **11** (2020) Article ID 571535 (18 pages); https://doi.org/10.3389/fphar.2020.571535

28. J. Guinney, R. Dienstmann, X. Wang, A. de Reyniès, A. Schlicker, C. Soneson, L. Marisa, P. Roepman, G. Nyamundanda, P. Angelino, B. M. Bot, J. S. Morris, I. M. Simon, S. Gerster, E. Fessler, F. De Sousa E. Melo, E. Missiaglia, H. Ramay, D. Barras, K. Homicsko, D. Maru, G. C. Manyam, B. Broom, V. Boige, B. Perez-Villamil, T. Laderas, R. Salazar, J. W. Gray, D. Hanahan, J. Tabernero, R. Bernards, S. H. Friend, P. Laurent-Puig, J. P. Medema, A. Sadanandam, L. Wessels, M. Delorenzi, S. Kopetz, L. Vermeulen and S. Tejpar, The consensus molecular subtypes of colorectal cancer, *Nature Med.* **21**(11) (2015) 1350–1356; https://doi.org/10.1038/nm.3967

29. R. Dienstmann, L. Vermeulen, J. Guinney, S. Kopetz, S. Tejpar and J. Tabernero, Consensus molecular subtypes and the evolution of precision medicine in colorectal cancer, *Nat. Rev. Cancer* **17**(2) (2017) 79–92; https://doi.org/10.1038/nrc.2016.126

30. K. C. G. Berg, P. W. Eide, I. A. Eilertsen, B. Johannessen, J. Bruun, S. A. Danielsen, M. Bjørnslett, L. A. Meza-Zepeda, M. Eknæs, G. E. Lind, O. Myklebost, R. I. Skotheim, A. Sveen and R. A. Lothe, Multi-omics of 34 colorectal cancer cell lines – a resource for biomedical studies, *Mol. Cancer* **16**(1) (2017) Article ID 116 (16 pages); https://doi.org/10.1186/s12943-017-0691-y

31. A. Sveen, J. Bruun, P. W. Eide, I. A. Eilertsen, L. Ramirez, A. Murumagi, M. Arjama, S. A. Danielsen, K. Kryeziu, E. Elez, J. Tabernero, J. Guinney, H. G. Palmer, A. Nesbakken, O. Kallioniemi, R. Dienstmann and R. A. Lothe, Colorectal cancer consensus molecular subtypes translated to preclinical models uncover potentially targetable cancer cell dependencies, *Clin. Cancer Res.* **24**(4) (2018) 794–806; https://doi.org/10.1158/1078-0432.ccr-17-1234

32. A. Okita, S. Takahashi, K. Ouchi, M. Inoue, M. Watanabe, M. Endo, H. Honda, Y. Yamada and C. Ishioka, Consensus molecular subtypes classification of colorectal cancer as a predictive factor for chemotherapeutic efficacy against metastatic colorectal cancer, *Oncotarget* **9**(27) (2018) 18698–18711; https://doi.org/10.18632/oncotarget.24617